

Supporting Information

Unlocking the Resistive Switching in Acacia Senegal-based Electrolyte for Neuromorphic Computation

Aziz Lokhandwala^{1,2}, Parth Thakkar^{1,2}, Jeny Gosai², Suvik Oza³ and Ankur Solanki^{1,2,*}

¹Department of Physics, Pandit Deendayal Energy University, 382426, Gandhinagar, Gujarat, India.

²Flextronics Lab, Pandit Deendayal Energy University, 382426, Gandhinagar, Gujarat, India.

³Department of Chemical Engineering, Pandit Deendayal Energy University, 382426, Gandhinagar, Gujarat, India.

*Email: ankur.solanki@sot.pdpu.ac.in.

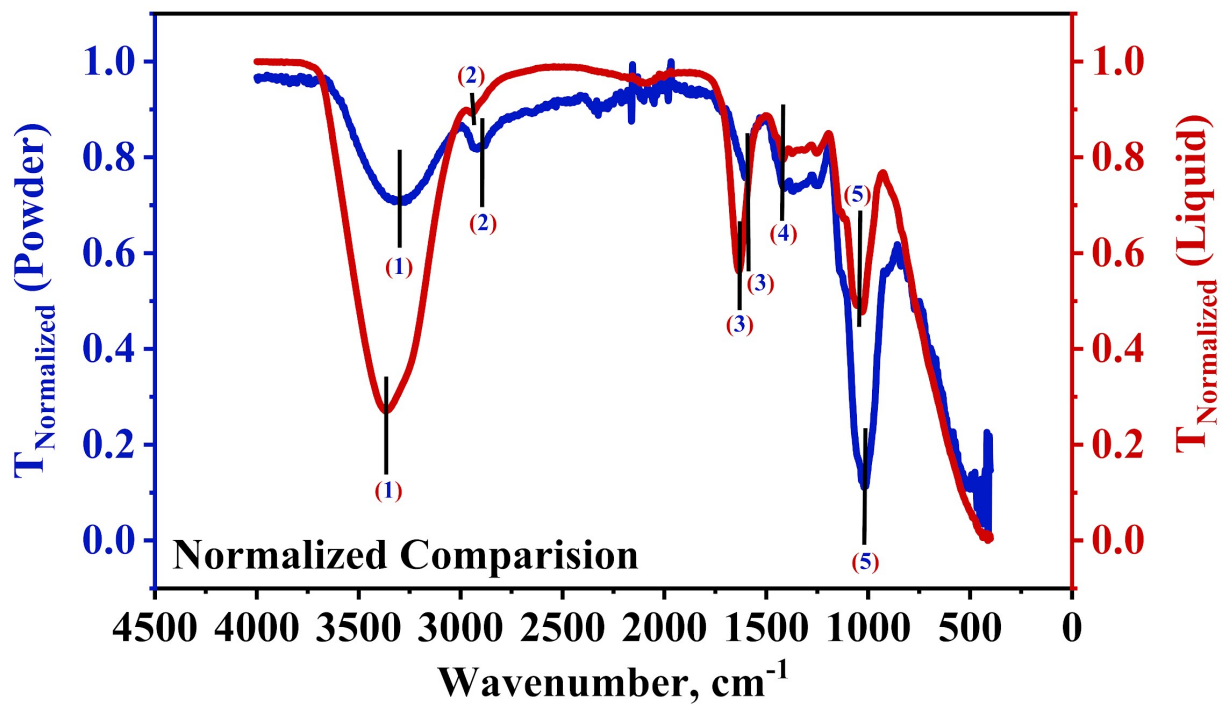


Figure S1: Normalized comparison of FTIR spectra of AS powder and AS@NaCl solution.

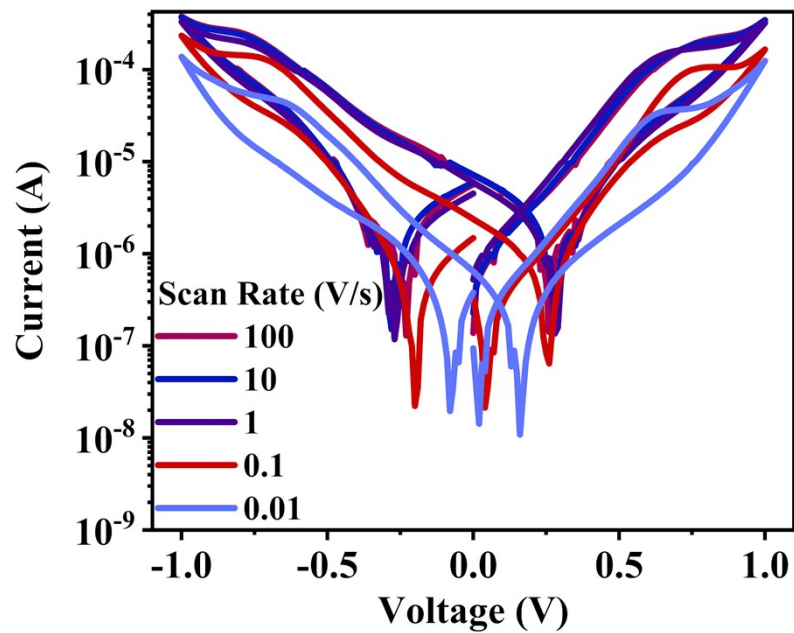


Figure S2: Variation in $\log I - V$ characteristics with scan rate (V/s). The current in the capacitor is proportional to the scan rate and is observed from the following figure.

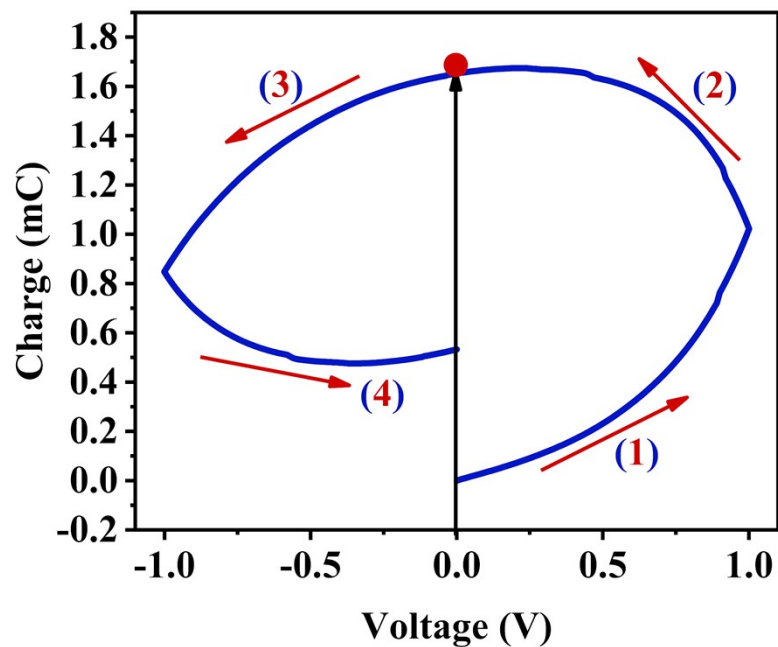


Figure S3: Charge-voltage characteristics obtained from the transient I-V characteristics, indicating a finite charge developed in the device after the complete voltage sweep ($0 \rightarrow 1 \rightarrow 0 \rightarrow -1 \rightarrow 0V$).

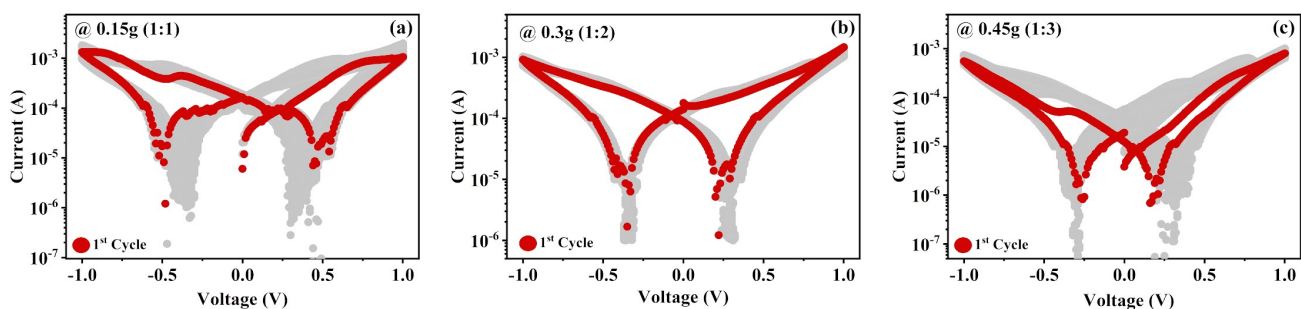


Figure S4: Cycle to cycle variation for 200 cycles for three different proportions (Salt : AS) of AS in 4.67M NaCl solution.

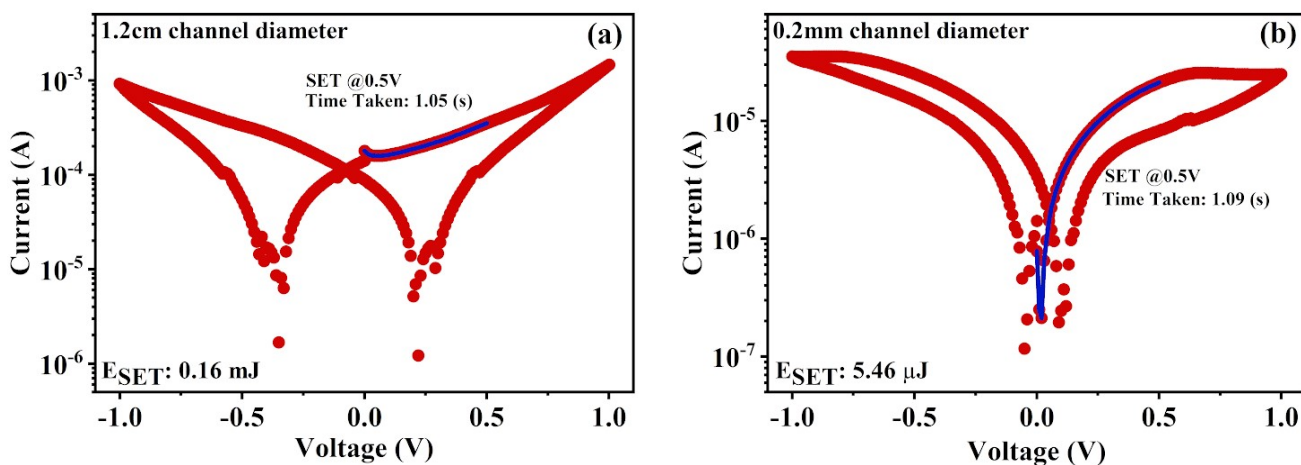


Figure S5: Energy consumption of device with two different channel diameters; (a) 1.2 cm, and (b) 0.2 mm. The consistent OFF/ON ratio of 4 is maintained in both of these configurations with scaling down of current and power consumption suggesting its possible applications for the cross bar architecture.

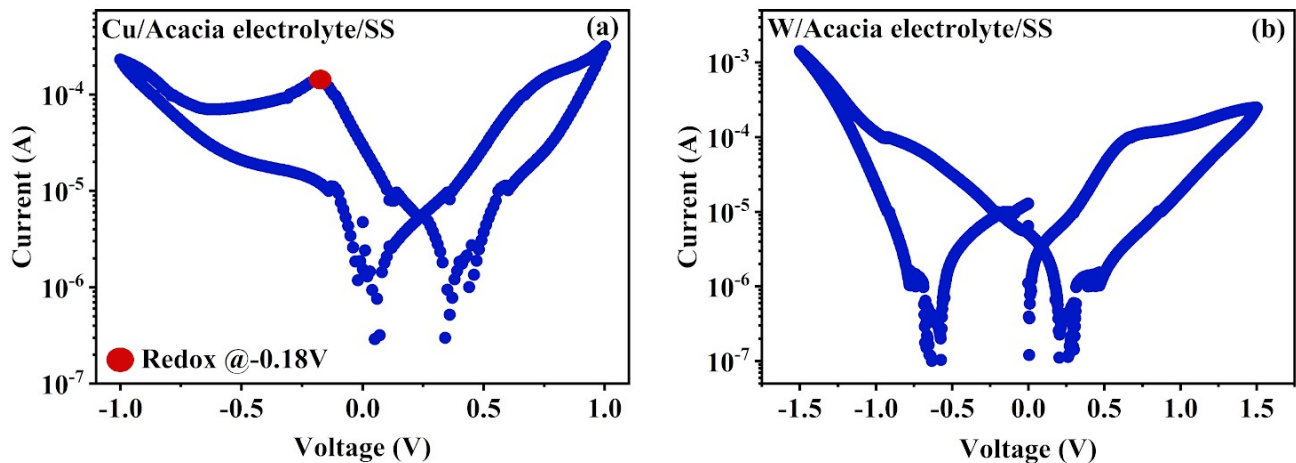


Figure S6: Semilog I-V characteristics for copper and tungsten electrodes with stainless steel (SS). (a) The oxidation of copper to Cu^{+2} has a standard oxidation potential of -0.34V . Because, the AS medium present here is acidic in nature ($\text{pH} \sim 4.5$), oxidation potential reduces to $\sim -0.20\text{V}$ at which oxidation of $\text{Cu}(\text{s})$ takes place. (b) For case of Tungsten replaced by the copper, the oxidation of it cannot take place due to its inert behaviour. The observed hysteresis is mainly due to ions in the AS@NaCl medium.

Calculation of Oxidation Potential of Cu in solution with $\text{pH} \sim 4.5$:

$$E_{cell} = E_{0,cell} - \frac{0.059}{n} \log[H^+]$$

Here n , is the number of electrons exchanged during oxidation reaction. For copper, $E_{0,cell} = -0.34, n = 2$ and $-\log[H^+] = \text{pH}_{AS}$. Using these values in above equation, E_{cell} turns out to be ~ -0.21 which is close to what we observe in Figure S5(a). Therefore, electrochemical metallization of Cu might be occurring in the Cu/AS@NaCl/SS.

Voltage (V)	R_s (Ω)		R_1 (Ω)		R_2 (Ω)		CPE (S, sec ⁿ)		n , ($0 < n < 1$)		C (F)	
	Low Frequency	High Frequency	Low Frequency	High Frequency	Low Frequency	High Frequency	Low Frequency	High Frequency	Low Frequency	High Frequency	Low Frequency	High Frequency
0.0	1113	49.17	1113	369	1113	9211	1E-5	1.45E-6	0.8	0.84	1E-5	9.47E-8
0.6	459.5	49.73	459.5	2588	459.5	2531	1E-5	1.87E-6	0.8	0.71	1E-5	9.93E-6
0.7	448.1	46.18	448.1	6.45	448.1	5271	1E-5	3.21E-6	0.8	0.85	1E-5	5.44E-4

Supplementary Table 1: The table shows values of circuit parameters at high and low frequency regimes. This also concludes the observation of series resistance of ~ 50 from the impedance data. The effect of capacitive double layer can be inferred from the n value for the Constant Phase element (CPE) which is close to 1 indicating capacitive behaviour of the double layer present at electrolyte-electrode interface. The R_1 and R_2 values correspond to the resistance values offered by the liquid electrolyte at low and high frequency counterparts.

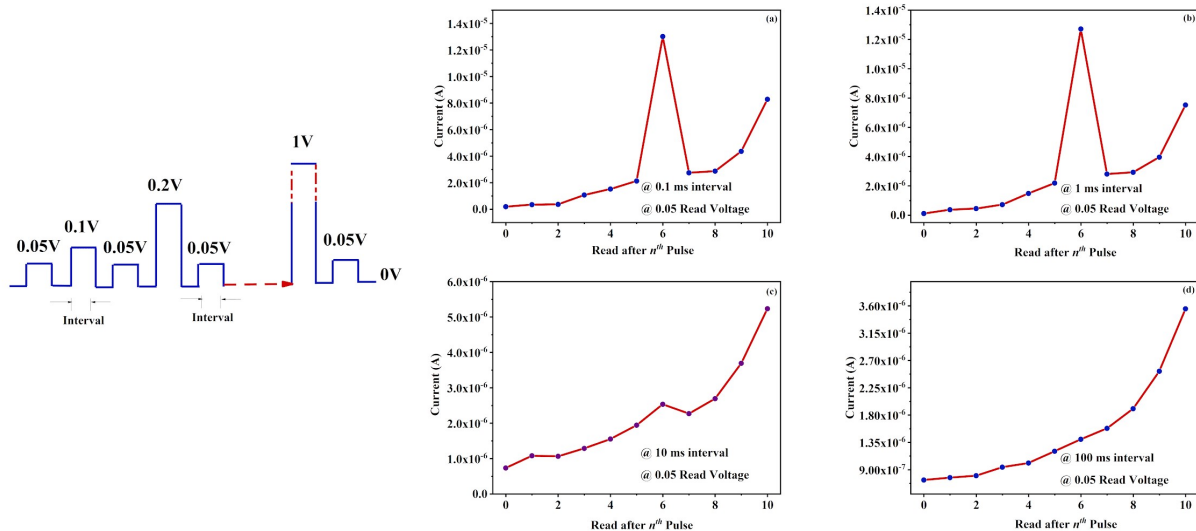


Figure S7: The data presented validates the plasticity characteristics of the device at read of 0.05 V. A sharp spike at 6th read pulse is indicating the read just after the SET voltage of 0.6V, vanishing with increasing pulse width (interval), as per the general plasticity behaviour exhibited by other memristor devices. (a) Plasticity at pulse width (interval) of 0.1 ms, (b) Plasticity at pulse width (interval) of 1 ms, (c) Plasticity at pulse width (interval) of 10 ms, and (d) Plasticity at pulse width (interval) of 100 ms.

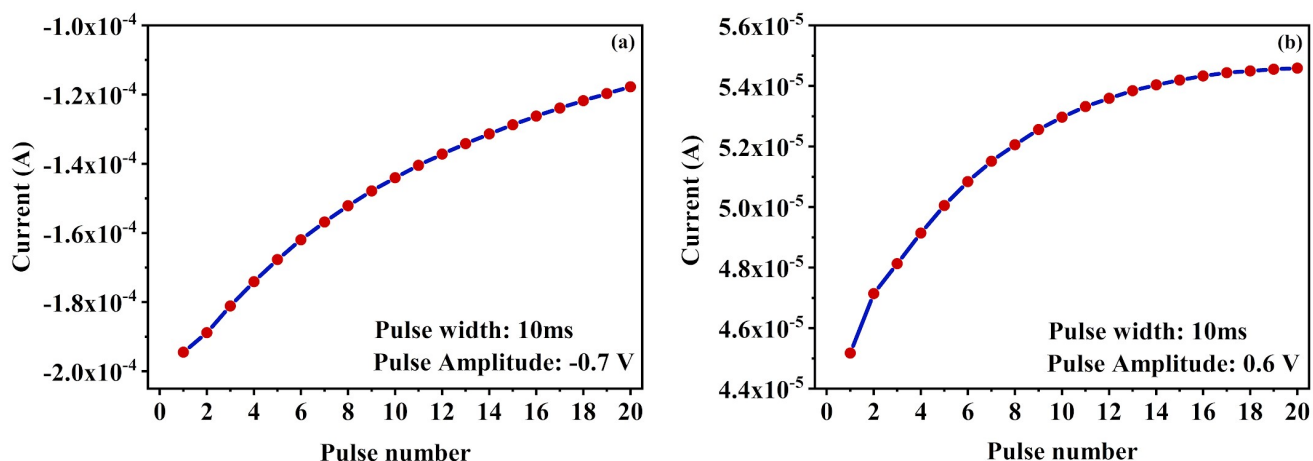


Figure S8: (a) Depression characteristics of the device with negative bias of -0.7 V with pulse width of 10 ms. (b) Potentiation characteristics of the device with a positive bias of +0.6 V and a pulse width of 10 ms.

Reason for the Observed Non zero current in zero bias and the Hysteresis in the I-V characteristics:

The effect of high concentration (4.67M) of NaCl in AS@NaCl is speculated to be the reason for the observed hysteresis in the *I-V* characteristics. The small angle X-ray scattering measurements for the AS@NaCl were presented in^[1] for different concentrations of NaCl. This study concludes the trade-off between electrostatic barrier due to negatively charged AS with the concentrations of NaCl. At higher concentration of NaCl, the electrostatic barrier is nearly absent within the bulk of the electrolyte, and is partly present at the electrode/electrolyte interface forming an electric double layer by the accumulation of OH⁻ and COO⁻ ions,^[3]^[4]. However, as the applied electric field across the device increases, the ions (Na⁺ and Cl⁻) present in the bulk traverses under the steric repulsion offered by the medium. This traversal also contributes to the shear thinning of AS. The shear thinning of AS contributes to an abrupt continuous decrease in the current in (1 → 0.6V) regime. Thence, the hysteresis in the I-V is attributed to the change in rheological property of the medium and the non-zero current at zero bias is due to the effect of the double layer.

Temperature dependence

Brookfield viscometer (model: LVDV2T; M/s Brookfield USA) is used to determine the viscosity of (Name of the sample) as shown in Figure S10 (a). 12g of NaCl was dissolved in 40 mL DI water to prepare a 4.67M solution. 24g of AS was dissolved in the prepared sample with heating at 75°C and continuous stirring at 350-400 rpm. Theand placed in the vial with an LV-61 spindle to check the viscosity. The spindle is connected to a motor for rotation. It is operated at a definite speed (50 rpm) and it is used to measure the resistance to the rotation of the flow. For temperature dependent I-V, an in-house setup was developed and the experiment was conducted.

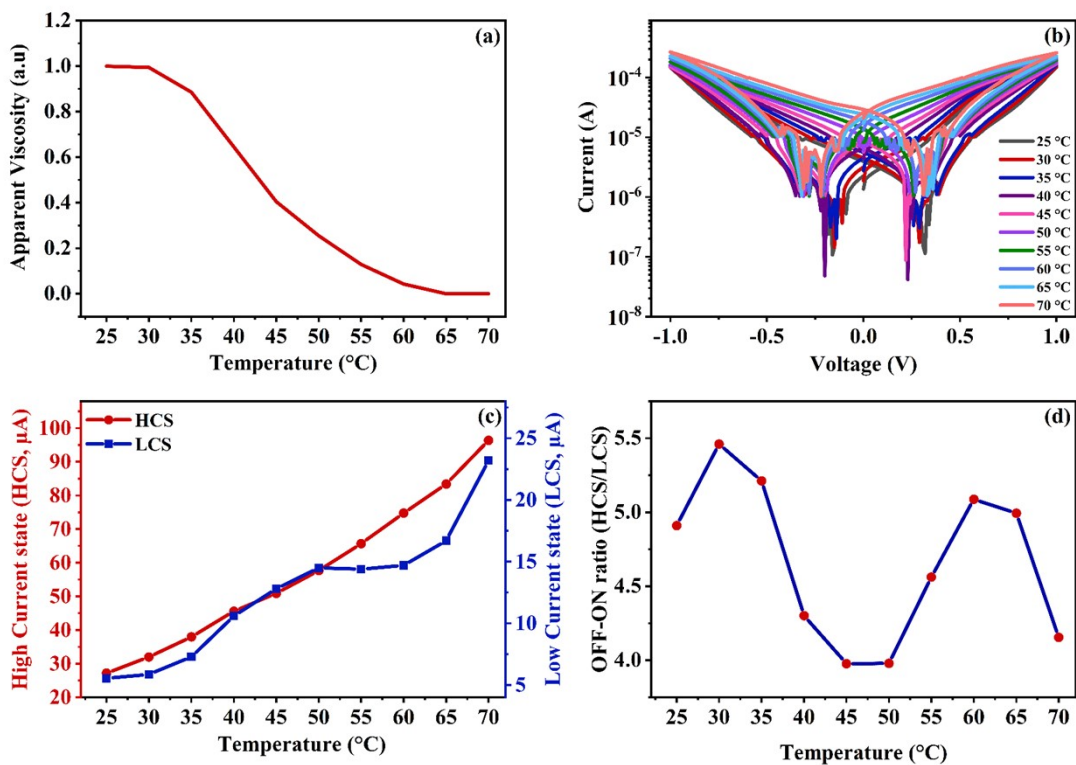


Figure S9: (a) Normalized viscosity plotted as a function of temperature. (b) I-V sweeps with variation of temperature in range (25 $^{\circ}\text{C}$, 70 $^{\circ}\text{C}$).

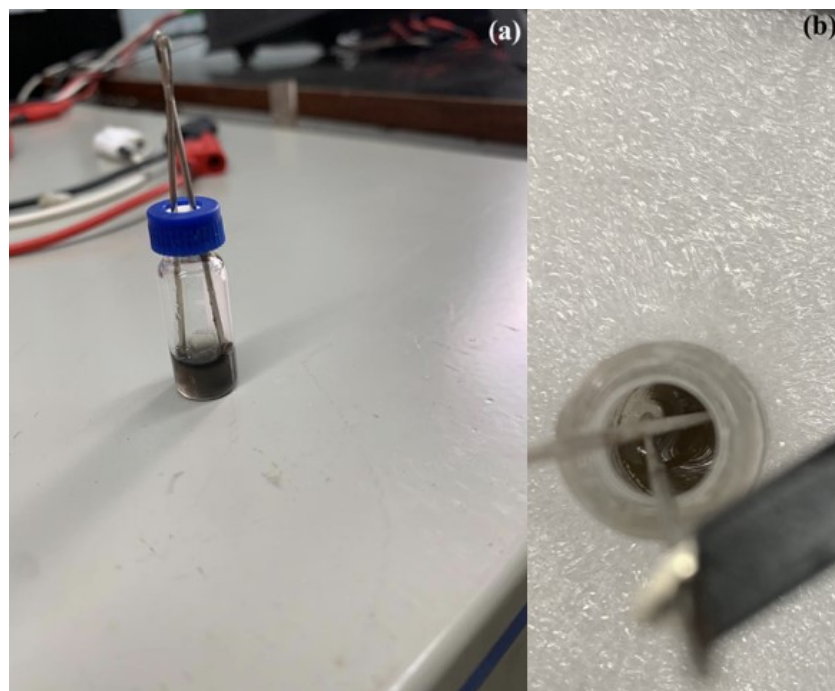


Figure S10: The resistive switching measurement setup. The device after applying high bias of 1.3V, indicating a thin blackish layer for the device breakdown. (b) Figure indicates the formation of chlorine gas bubbles at one of the electrodes, validating the proposed mechanism for resistive switching.

References:

- [1] Dror, Y., Cohen, Y. and Yerushalmi-Rozen, R. (2006), Structure of gum arabic in aqueous solution. *J. Polym. Sci. B Polym. Phys.*, 44: 3265-3271. <https://doi.org/10.1002/polb.20970>.
- [2] P.A. Williams, G.O. Phillips, 11 - Gum arabic, Editor(s): G.O. Phillips, P.A. Williams, In Woodhead Publishing Series in Food Science, Technology and Nutrition, Handbook of Hydrocolloids (Second Edition), Woodhead Publishing, 2009, Pages 252-273, ISBN 9781845694142, <https://doi.org/10.1533/9781845695873.252>.
- [3] Ullah R, Khan N, Khattak R, Khan M, Khan MS, Ali OM. Preparation of Electrochemical Supercapacitor Based on Polypyrrole/Gum Arabic Composites. *Polymers*. 2022; 14(2):242. <https://doi.org/10.3390/polym14020242>.
- [4] Khalid, M., Honorato, A.M.B. Ionically conducting and environmentally safe gum Arabic as a high-performance gel-like electrolyte for solid-state supercapacitors. *J Solid State Electrochem* **21**, 2443–2447 (2017). <https://doi.org/10.1007/s10008-017-3585-4>.